



ORDER FILTERING OF ROTATING MACHINERY OPERATIONAL RESPONSE DATA USING WAVELET PACKET DECOMPOSITION AND RESAMPLING TECHNIQUES

Ramon Fuentes¹, Trevor Walton²

ABSTRACT

The identification and removal of rotor harmonics from in-flight operational data provides a key to the analysis of helicopter dynamics. This paper presents a technique for harmonic removal from operational structural response data with little or no effect on the underlying dynamic properties represented by the signal.

The filter-bank structure of the Wavelet Packet Decomposition (WPD) can be used together with revolution domain resampling and multi-rate signal processing in order to extract harmonic components from the operational response of rotating machinery. The bandwidth of each of the sub-bands of a WPD at a given level is dependent on the initial sampling rate of the signal. The signal can be resampled such that the base frequency of the harmonic to be extracted lies exactly in the overlap between two sub-bands. The effect of this is that components of the base frequency and its harmonics will be aliased and will appear as constant offsets within the two sub-bands adjacent to the base frequency as well as all of its harmonics. This offset can be determined and removed from either all or selected sub-bands, which results in the extraction of all or selected harmonics from the original signal after the inverse WPD is applied.

Keywords: Conference, Operational, Modal, Analysis, Harmonics, Filter, Removal, Wavelet

¹ R&D Engineer, HBM- nCode, ramon.fuentes@hbmncode.com

² Vibration Specialist, AgustaWestland, Trevor.Walton@agustawestland.com

1. INTRODUCTION

1.1. Motivation – Operational Modal Analysis in Rotary Wing Aircraft

The motivation for the development of this method is to be able to undertake Operational Modal Analysis (OMA) on the operational response of rotary wing aircraft structures. The presence of harmonics has been clearly identified as a major difficulty in undertaking OMA in rotating machinery [1, 2, 3, 4, 5]. Several methods have been suggested for this task which include time domain and angle domain synchronous averaging [1, 2, 6]. A method for the removal of stationary harmonics was presented in [7] based on wavelet denoising techniques [8]. This was later extended to use multi-rate signal processing techniques in [9], and extended to perform combined harmonic removal and signal denoising in [10]. These methods work well for the removal of stationary harmonics, but the challenge OMA sets on rotating machinery is the removal of largely nonstationary signals. The method presented here builds on [9] to develop a filter used to remove nonstationary harmonic components of a signal. It makes use of revolution domain resampling and wavelet analysis to remove the harmonics, with no distortion to the underlying original signal.

1.2. Time-Frequency vs. Time-Scale Analysis

1.2.1. Time-Frequency Analysis

The Fourier Transform provides a frequency representation of a signal by assuming that it is composed of sines and cosines of infinite length and constant frequency. It is then, in principle, not suitable for the analysis of non-stationary signals. The Short Time Fourier Transform (STFT) [11] addresses this issue by analysing sections of the signal on a sliding window. There is, however, an inherent compromise between the time and the frequency resolution when specifying a window size in the STFT. The Gabor Transform [12] builds on the STFT by windowing the periodic basis function which deals with the fact that the signal sections are not of infinite length. Time-frequency analysis methods work well for a wide range of practical situations. However, the signal is still assumed to be stationary within each window, which renders STFT and the Gabor Transform unsuitable for signals where the transients are very significant.

1.2.2. Time-Scale Analysis

The Continuous Wavelet Transform (CWT) [13, 14, 15] is an extension of the STFT and Gabor Transform. The idea behind the CWT is to represent the signal through translations and dilations of the basis function, or mother wavelet. The translation operation specifies time localization, in a similar way to STFT, while the dilation specifies the “scale”, which is related to the frequency. For this reason we talk about time-scale analysis. Large scales correspond to low frequencies and vice-versa. The CWT is defined as

$$X_{\psi}(a, b) = \frac{1}{\sqrt{a}} \int_{-\infty}^{+\infty} x(t) \psi * \left(\frac{t-b}{a} \right) dt \quad (1)$$

where a is the scale or dilation, b is the translation parameter, ψ is the mother wavelet and $*$ denotes complex conjugation.

The computation of the CWT will consume significant time and resources. A faster and more efficient algorithm is the Discrete Wavelet Transform (DWT) [15, 16, 13] which uses digital filtering techniques to obtain a time-scale representation of the signal. The digital filters are implemented as

filter banks, as shown in Figure 1. The filter bank structure of the DWT uses a low pass and a high pass filter at each level. These split the signal into the “approximation” and “detail” wavelet coefficients, containing the low and high frequency components of the signal, respectively. Each filtering operation is followed by decimation, which halves the number of samples at each level. This decimation will be key in the removal of harmonics. The DWT is defined as

$$X_n^m = \int_{-\infty}^{+\infty} x(t)\psi_{m,n}(t) dt \quad (2)$$

where $\psi_{m,n}(t)$ are discrete sets of the mother wavelet which have been translated and dilated according to a dyadic grid:

$$\psi_{m,n}(t) = 2^{m/2}\psi(2^m t - n) \quad (3)$$

where,

$$a = 2^{-m}, b = n2^{-m} \quad (4)$$

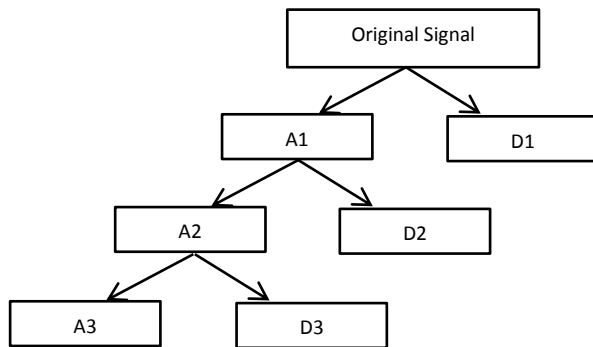


Figure 1 – Structure of the DWT. The approximation and detail coefficients for level i are labeled A_i and D_i respectively. Note that for an n level DWT, the whole spectrum of the signal is captured with coefficients $D_1, D_2, \dots, D_n, A_n$.

1.3. Aliasing of harmonics

The signal containing harmonics can be represented as

$$x(t) = y(t) + R(t) = y(t) + \sum_{k=1}^L R_k(t) \quad (5)$$

Where the $R(t)$ contains L harmonics of a base frequency.

$$R_k(t) = \sum_{k=1}^L a_k \sin(2\pi f_k t + \phi_k) \quad (6)$$

Where a_k, f_k and ϕ_k are the amplitude, frequency and phase of the k^{th} harmonic. After the application of the DWT down to level J , the wavelet coefficients for $x(t)$ can be expressed, for every sample i as

$$d_J[i] = d_{y_J}[i] + d_{R_J}[i] \quad (7)$$

By examining Figure 1 we can see that we can arrive at d_J through a cascade of J half-band filters with a decimation by 2 at every level. We are interested in the effect that this filtering and decimation down to level J has on the harmonics. To examine this, we can consider the DWT down to level J as equivalent to applying a bandpass linear filter, ψ_J followed by decimation by 2^J . The harmonic components expressed in terms of wavelet coefficients are thus

$$d_{R_J} = R * \psi_J \quad (8)$$

where $*$ denotes convolution. Since ψ_J is a linear filter, the harmonics remain periodic after the filtering.

$$d_{R_J}[i] = \sum_{k=1}^L a'_k \sin(2\pi f_k t_i + \phi'_k) \quad (9)$$

where a'_k and ϕ'_k are the amplitude and phase of d_{R_J} , which depend on the frequency and phase response of ψ_J . The term t_i is the result of decimation:

$$t_i = \frac{2^J i}{F_s} \quad (10)$$

where F_s is the original sampling rate of the signal. Now, if we choose F_s to be

$$F_s = F_h \times 2^J \quad (11)$$

where F_h is the base frequency of all the harmonics in R , we can observe the effect that this has on the harmonics by substituting (11) and (10) into (9),

$$d_{R_J}[i] = \sum_{k=1}^L a'_k \sin(2\pi k i + \phi'_k) = \sum_{k=1}^L a'_k \sin(\phi'_k) \quad (12)$$

since k and i are integers the product $2\pi k i$ equates to 0, so that the term is now a constant. Through the choice of a sampling rate that meets (11), the harmonics can be completely aliased on the J^{th} level of the DWT.

As an illustration we take 2 signals, both sine-on-random containing a single harmonic at 5 Hz. The first signal is sampled at 90 Hz and the second one is sampled at 80Hz. We then take the DWT of these signals down to 4 levels and observe the effect of the different sampling rates. Since $J=4$, we can see that the second signal sampled at 80Hz meets (11), since $5 \times 2^4 = 80$. So we would expect the detail coefficients on the 4th level not to be periodic. This is illustrated in Figure 2

The procedure for the removal of harmonics presented in [9] is to estimate this offset, and subtract it from the respective wavelet coefficients, followed by an inverse DWT. This procedure has been extended here as will be explained in Section 2.3 .

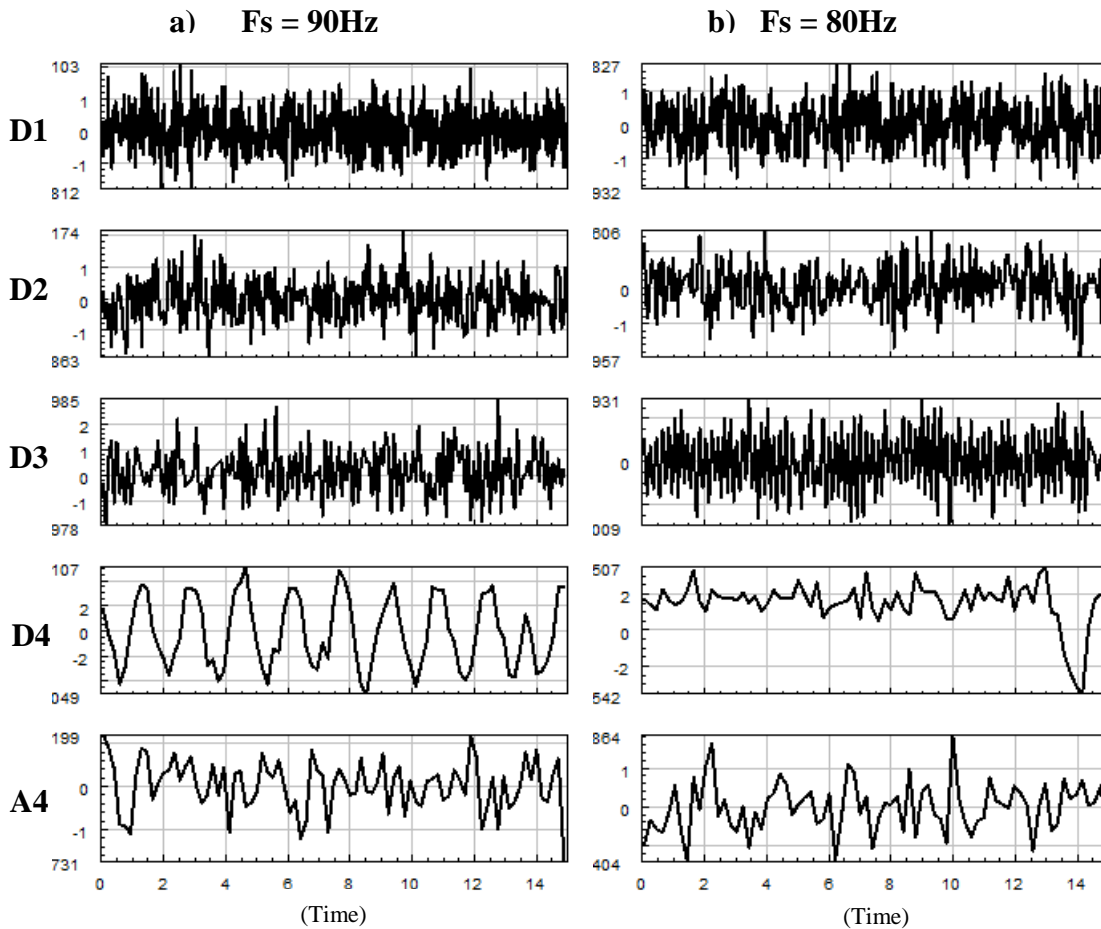


Figure 2 – DWT down to 4 levels applied to two signals composed of white noise and a sine tone at 5 Hz. a) was sampled at 90 Hz, b) is sampled at 80 Hz and meets the condition for a harmonic appearing as offset. Note how the coefficients in D4 are periodic in a), while an offset is evident in b).

2. REMOVAL OF HARMONICS

2.1. Revolution Based Re-Sampling

The method presented here makes use of the revolution-based resampling technique. This is a resampling technique that transforms signals sampled at constant time intervals into an angular domain, based on an RPM signal derived from a tachometer that is phase-locked with the signals in question. The re-sampled signal will contain the harmonics at a fixed and known frequency, easing the process of removal.

In the case of rotary wing aircraft, for example, the RPM signal is derived from a tachometer placed on the main rotor. In the time domain, the rotor harmonics are multiples of the main rotor speed. When resampled into the revolutions domain, the main rotor speed is always 1 revolution, so the dominant harmonics will always be integer multiples of 1 revolution, making them easier to identify and remove. Once the necessary filtering is done to the signals, these can be resampled back into the time domain.

2.2. Use of Wavelet Packet Decomposition (WPD)

Section 1.2 introduced the DWT as a filter bank structure that splits the signal into a low and high frequency part recursively. This leads to the effect of harmonics appearing as a DC offset in the wavelet coefficients through the application of digital filters and decimation, as explained in section 1.3.

There is another filter bank structure, similar to the DWT, called Wavelet Packet Decomposition (WPD) [15, 14] which is useful since it splits the spectrum of the signal into even “sub bands” of equal bandwidth. Figure 3 shows the binary tree structure of the WPD. Each of the nodes in the tree of the WPD contains a set of wavelet coefficients. The filter bank is constructed through filtering and decimation in a similar way to the DWT. Thus, the harmonics can be aliased through the same sampling condition (11) as discussed in Section 1.3.

The practical advantage of the WPD over the DWT for the purpose of removing harmonics is the equal bandwidth of the nodes. This means that all of the harmonics of a base frequency can be removed by removing the baseline on all the nodes. This is the approach taken in [9].

The WPD also exhibits less leakage of energy from harmonics into adjacent sub-bands. This makes possible the removal of a single sine tone from the signal (as opposed to a sine plus all its harmonics), through the selection of a mother wavelet with a sharp frequency roll-off, and selection of the appropriate sub-bands.

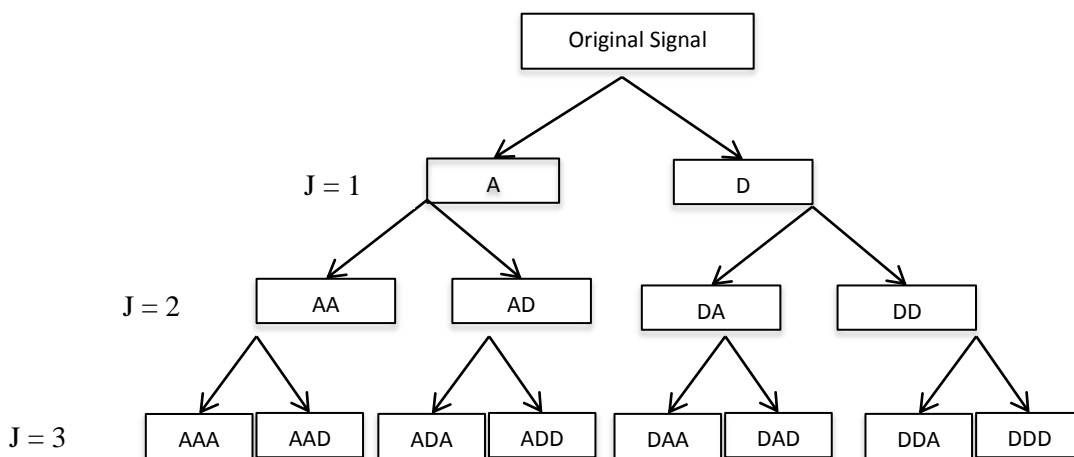


Figure 3 – Filter bank structure of the Wavelet Packet Decomposition (WPD).

2.3. Removal of DC Offset on Wavelet Coefficients.

Revolution based resampling solves the problem of the slight variations in main rotor frequency associated with rotary wing aircraft, and rotating machinery in general. With the signals sampled in an angular domain, they can be upsampled to the next sampling rate that meets (11) in order for the harmonics to be aliased under the wavelet coefficients of an appropriate level. The basic procedure for harmonic removal, outlined in [9], is to resample the signal to a sample rate that meets (11), apply a wavelet decomposition, estimate the offset caused by the harmonics (which will be the mean of the wavelet coefficients if the original signal has zero-mean), remove that offset and apply an inverse wavelet transformation.

Estimating the mean of the wavelet coefficients and removing it will completely cancel out the harmonics if the harmonics are of constant amplitude. This is a direct consequence of equation (12),

where it can be seen that the value of the constant representing a harmonic component within a set of wavelet coefficients is dependent on the amplitude of the original harmonic. In other words, if the amplitude of the harmonics in the original signal varies with time, the DC offset, as seen through the wavelet coefficients will also change. Thus, if the signal contains transient harmonics and one attempts to remove these through baseline shifting of the wavelet coefficients, this will result in an incomplete removal of the harmonics.

The solution adopted by the authors is to estimate the running mean of the wavelet coefficients, and to subtract it from the wavelet coefficients. This, followed by an inverse wavelet transform, results in complete removal of the transient harmonics. However, it requires careful selection of the window size used in the estimation of the running mean. The effect of transients in the wavelet coefficients is illustrated in

Figure 4. This illustrates the use of the running mean, and how transients in amplitude of the harmonics affect the variation of the DC offset on the wavelet coefficients. Formally speaking, a running mean is a simple finite impulse response (FIR) filter, so the running mean or moving average is the convolution between the wavelet coefficients and a square window

$$M_{J,P}[i] = d_{J,P}[i] * \Phi \quad (13)$$

where $M_{J,P}[i]$ is the moving average of wavelet coefficients $d_{J,P}[i]$ at level J and sub-band P . The square window is Φ and $*$ denotes discrete convolution. The coefficients $d_{J,P}[i]$ are then substituted by the new ones:

$$d'_{J,P}[i] = d_{J,P}[i] - M_{J,P}[i] \quad (14)$$

The coefficients $d'_{J,P}[i]$ are then used in the inverse wavelet transform in order to arrive at the filtered signal in the time (or in this case, angular) domain.

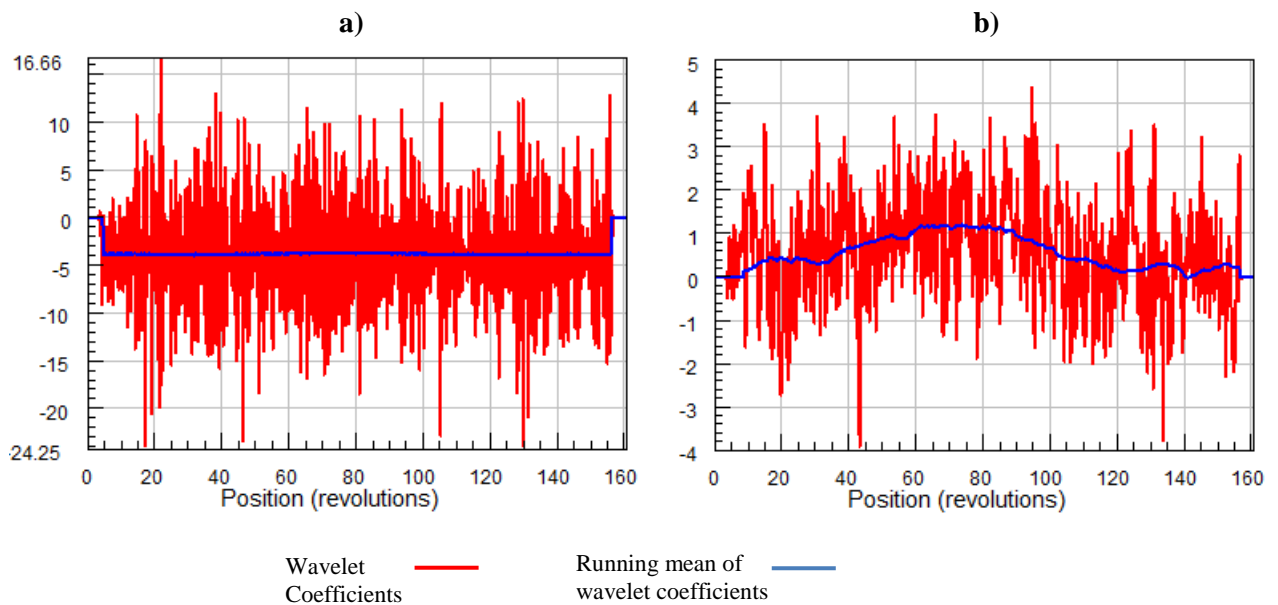


Figure 4 – Wavelet coefficients of the relevant sub-bands for a helicopter signal containing harmonics and sampled at a condition that meets (11). Signals for two different events are shown a) rotor harmonics have largely constant amplitude, b) Rotor harmonics exhibit transients in amplitude.

3. VALIDATION USING A 3-DOF MSD SYSTEM SIMULATION

This section demonstrates the application of the wavelet harmonic filter to the response of a 3 degrees-of-freedom (DOF) mass-spring-damper (MSD) system numerical model. The objective is to compare the response of the system to a sine-on-random excitation, with the harmonics removed using the methods described in this paper against the system's response to only the white noise component. The results can be seen in Figure 5 in the frequency domain and Figure 6 in time domain.

1.1 Methodology

The system simulated was a basic mass-spring-damper with the masses connected in series and grounded on both ends. The parameters used were the same for all masses, springs and dampers. These were $m = 10$ kg, $k = 10000$ N/m and a damping ratio of 0.01. Two simulations were produced in order to compare the response of the system to pure white noise excitation, against the *filtered* response of the system to a sine on random excitation. The sine tones were placed at 5,10 and 20 Hz. All runs were of 300 seconds and used the exact same white noise excitation.

The simulated excitations were sampled at 512 Hz. For the purpose of comparing the data like-for-like, all filtered signals were resampled back to 512 Hz before applying the FFT. All FFTs were applied with a Hanning window, 67% overlap and 2048 spectral lines (yielding a frequency resolution of 0.125 Hz). The first and last second of data were removed from all signals in order to compare results without the presence of edge effects.

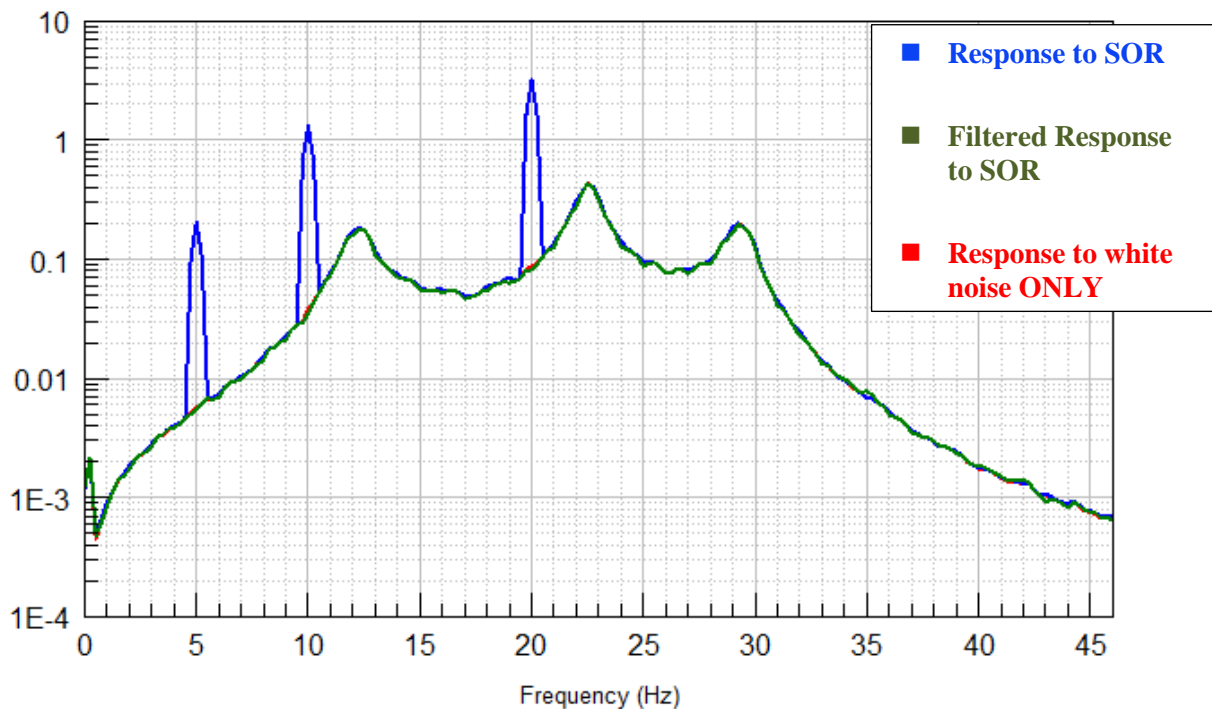


Figure 5 – Application of the harmonic filter to the removal of three sine tones from a simulated response to a 3-DOF system (green). This response is compared to the response of the system to white noise excitation (red). It can be seen that the filtered response matches the response to white noise.

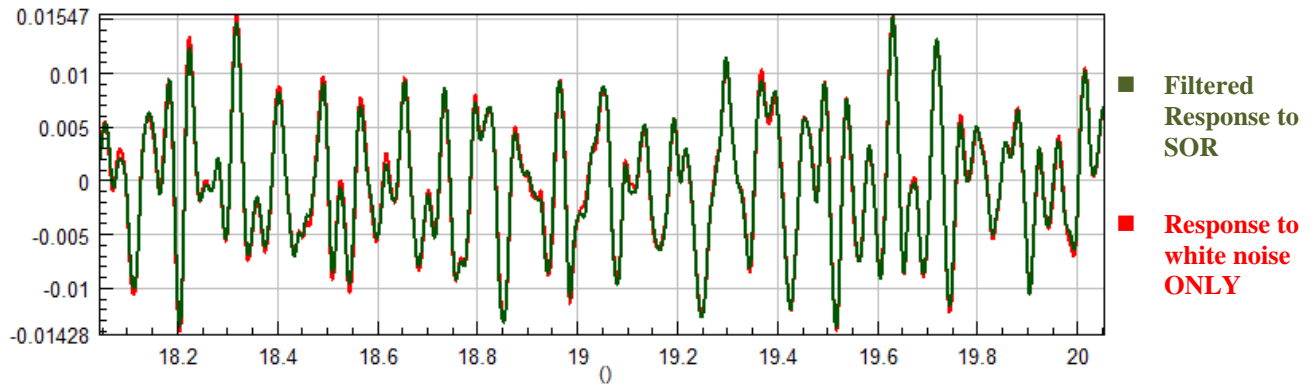


Figure 6 – Time domain comparison of the 3-DOF system results. Only the filtered response (green) and the response to white noise are shown (red). It can be seen that even in the time domain, the filtering has very little distortion.

4. RESULTS ON HELICOPTER FLIGHT TEST DATA

Figure 8 shows the results of the method presented here, used to remove all harmonics of the main rotor from the measured response of a helicopter. The example clearly shows how the underlying structural resonance is not affected by the removal of the harmonics around it.

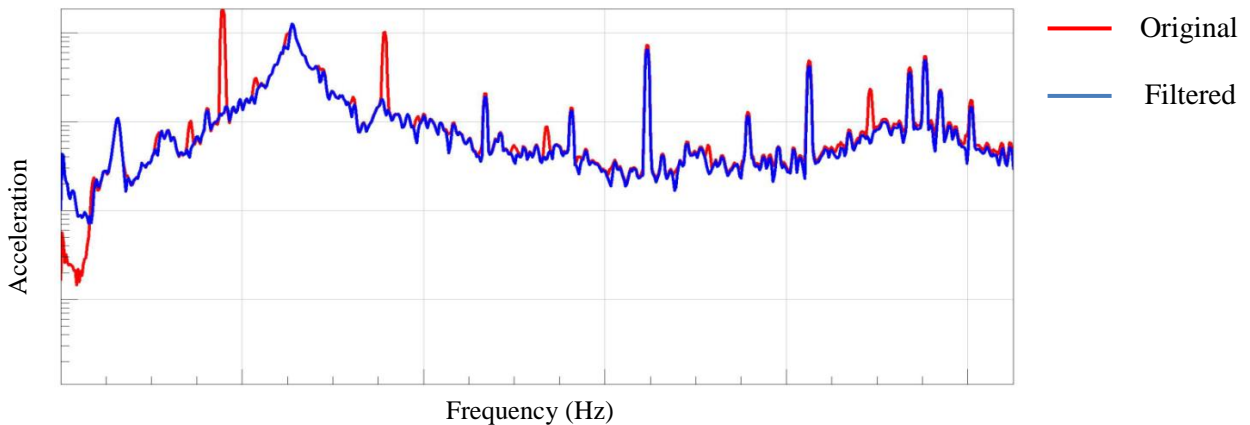


Figure 7 – Result of applying the filter to all of the nodes to remove all harmonics of the main rotor of a helicopter. This example shows how this method removes the harmonics without interfering with the underlying dynamics. Note that the harmonics that are left are not harmonics of the main rotor.

5. CONCLUSIONS

A method for removal of harmonics from operational response signals on rotating machinery has been presented. It is based on revolution domain resampling and wavelet analysis. The filtering method has been validated through numerical simulations of a mass-spring-damper system.

The method has also been applied to in-flight response data of a helicopter. This application has

yielded very positive results. It can completely remove all or selected harmonics while leaving the underlying structural dynamics represented by the signals with little or no distortion.

ACKNOWLEDGEMENTS

This work was funded by AgustaWestland as part of their research initiative into Operational Modal Analysis. The authors wish to acknowledge Rob Plaskitt and Andrew Halfpenny of HBM-nCode for their valuable input throughout the development of this method, as well as Elizabeth Cross and Keith Worden from The University of Sheffield.

REFERENCES

- [1] B. Peeters, et al, "Removing Disturbing Harmonics in Operational Modal Analysis," in *IOMAC Conference*, Copenhagen, Denmark, 2007.
- [2] Jacobsen, N.J., "Eliminating the Influence of Harmonic Components in Operational Modal Analysis," in *IMAC XXV*, 2007.
- [3] N.-J. Jacobsen, "Separating Structural Modes and Harmonic Components in Operational Modal Analysis," in *IMAC XXIV*, 2006.
- [4] P. Mohanty, "Operational Modal Analysis in the presence of harmonic excitations, PhD Thesis," T.U. Delft, The Netherlands, 2005.
- [5] Cavagnino, C., "Operational modal analysis of a lightweight helicopter tail," in *LMS Conference*, Germany, 2006.
- [6] C.L. GROOVER, M.W. TRETHERWEY, K.P. MAYNARD AND S.M. LEBOLD, "Removal of order domain content in rotating equipment signals by double resampling," *Mechanical Systems and Signal Processing*, vol. 19, no. 3, pp. 483-500, 2005.
- [7] Xu, Lijun; Yan, Yong, "Wavelet Based Removal of Sinusoidal Interference from a Singal," 2004.
- [8] Donoho, David L., "Denoising by Soft Thresholding," *Department of Statistics, Stanford University*.
- [9] Xu, Lijun, "Cancellation of Harmonic INterference by Baseline Shifting of Wavelet Packet Decomposition Coefficients," vol. 53, no. 1, 2005.
- [10] Han, Jun; Hao, Ying; Xu, Lijun, "Simultaneous Removal of Harmonic Interference and White Noise by Combining Multi-Rate Signal Processing Techniques and Wavelet Denoising Techniques," Warsaw, Poland, 2007.
- [11] S. Qian, D. Chen, *Joint Time–Frequency Analysis: Methods and Applications*, Prentice-Hall, 1996.
- [12] W.J. Wang, P.D. McFadden, "Early detection of gear failure by time–frequency analysis. Part 1: Calculation of the time–frequency distribution," *Mechanical Systems and Signal Processing*, vol. 7, pp. 193-204, 1993.
- [13] Graps, A., "An Introduction to Wavelets," vol. 2, no. 2, 1995.
- [14] Hubbard, B.B., *The World According to Wavelets: The Story of a Mathematical Technique in the Making*, A.K. Peters, 1998.
- [15] Vetterli, Martin, "Wavelets and Filter Banks: Theory and Design," vol. 40, no. 9, 1992.
- [16] D. T. Lee and A. Yamamoto, "Wavelet Analysis: Theory and Applications," 1995.